JACS
JOURNAL OF THE AMERICAN CHEMICAL SOCIETY
Article
Cite This: J. Am. Chem. Soc. 2018, 140, 167−175
pubs.acs.org/JACS

Activity of Tumor Necrosis Factor α Is Modulated by Dynamic Conformational Rearrangements

Daniela Hofmann, Loïc Salmon, and Gerhard Wider*

Institute of Molecular Biology and Biophysics, ETH Zürich, 8093 Zürich, Switzerland

Supporting Information

ABSTRACT: The homotrimeric ligand tumor necrosis factor α (TNFα) is a key cytokine and immune regulator; however, when deregulated, it leads to several major chronic inflammatory diseases. Perturbation of the protein−protein interface has proven to be an efficient strategy to inactivate TNFα, but the atomic-resolution mechanism of its inactivation remains poorly understood. Here, we probe the solution structure and dynamics of active and inactive TNFα using NMR spectroscopy. The data reveal that TNFα undergoes motions on different time scales. Furthermore, by site-directed mutagenesis of residues at the trimerization interface and by targeting the interface with a low molecular weight inhibitor, we show that TNFα retains its overall structure and trimeric state. However, upon perturbation, TNFα exhibits increased conformational dynamics spanning from the trimerization interface to the regions mediating receptor binding. These findings provide novel insights into the inactivation mechanism of TNFα and the basis for strategies to target TNFα activity.

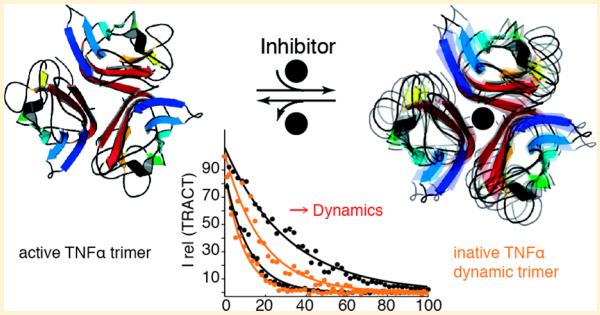

INTRODUCTION

Since its discovery as an antitumor agent, half a decade ago, tumor necrosis factor α (TNFα) has enjoyed enormous scientific and pharmaceutical interest, constantly renewed due to its pivotal role in the immune response and its relationship to many human diseases. Deregulation of TNFα is associated with several human malignant conditions including rheumatoid arthritis, Alzheimer's disease, psoriasis, inflammatory bowel disease, major depression, and cancer.[1−6]

TNFα belongs to the TNFα superfamily of ligands, which are characterized by a conserved architecture, the TNFα homology domain (THD), and exert their biological function by a common binding mode to their cognate receptors TNFR1 and TNFRF2.[6−8] In vivo, active TNFα is an obligate homotrimeric complex and its dissociation leads to a loss of function.[9,10] Site-directed mutational analysis of TNFα indicates that regions important for bioactivity comprise residues mediating receptor binding as well as residues involved in formation of the trimerization interface.[11,12] Mutants containing substituted residues at the protein−protein interface (PPI) showed drastically reduced receptor-binding capabilities that abolished the TNFα response. Over the past years, the mechanism of TNFα inactivation has been intensively disputed. Studies have shown that deoligomerization manifests itself in diminished TNFα signaling, possibly due to weaker recruitment of TNFRs, while others propose that disruption of the trimer is not a prerequisite for attenuated activity.[9,11−13] However, no detailed molecular model supports this notion, and therefore the mode of inactivation remains elusive.

Crystallographic data for native TNFα reveal that each monomer of the trimeric THD comprises two β-sheets, each consisting of five antiparallel β-strands. The inner and outer sheets form together a jelly roll topology (Figure 1A). The terminal strands of both sheets of one monomer interact with the inner sheet of the adjacent monomer and in such a way assemble the trimeric THD. The interface is composed mainly of hydrophobic amino acids and involves a cluster of aromatic residues including Y119 and Y59. TNFα harbors one disulfide bond linking the two top loops 3 and 4 (TL3 and TL4 in Figure 1A), giving rise to an overall pyramidal shape.[14,15] When binding to its receptor, TNFα triggers downstream signal cascades.[2] The binding is mediated via interactions between conserved cysteine-rich domains of the receptor and the intersubunit groove of trimeric TNFα, which is defined by residues from TL1, TL2, and bottom loop 4 (BL4)[17,18] (Figure 1A).

The fact that the activity of TNFα can be abolished allosterically by interfering with the PPI generates immense therapeutic perspectives. Significant breakthroughs were obtained by successfully targeting TNFα with antibodies.[19−23] However, these large molecules provoke major side effects and cause immunogenicity.[24] The development of new TNFα blockers, which defeat the immunogenicity issues and with potentially attenuated side effects, is crucially needed.[25−27] Small-molecule inhibitors would be preferable and currently attract enormous attention as alternative TNFα blockers.[25] Recently a number of small-molecule inhibitors interfering with

Received: May 16, 2017
Published: December 1, 2017

DOI: 10.1021/jacs.7b05050
J. Am. Chem. Soc. 2018, 140, 167−175

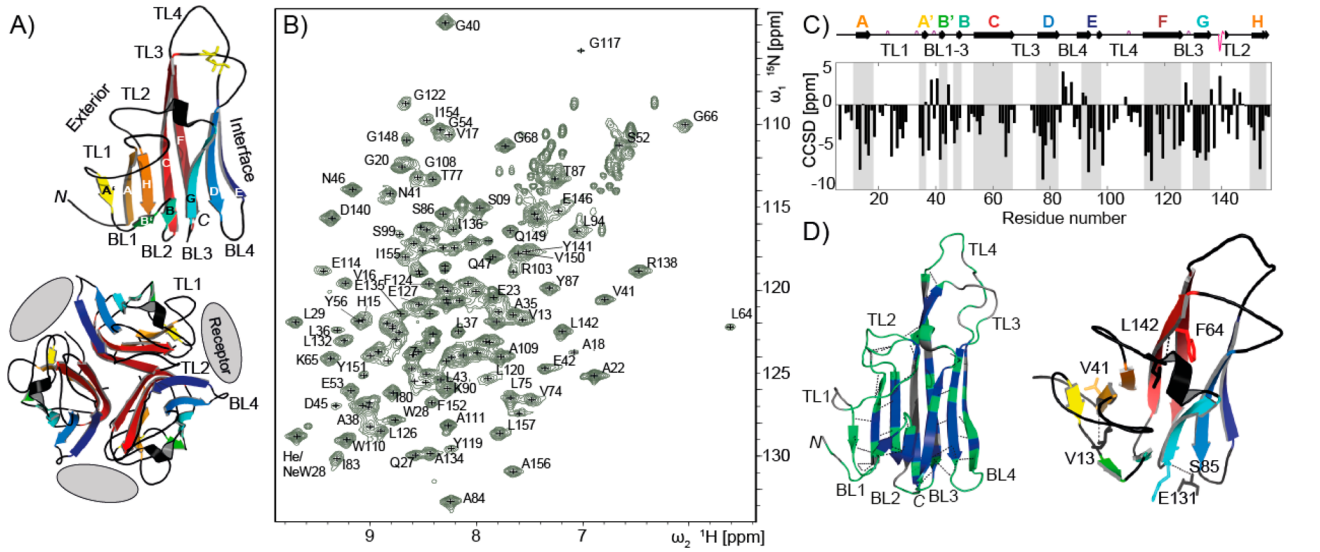

Figure 1. TNFα adopts a similar fold in solution as in the crystal. (A, top) Sketch of TNFα based on the crystal structure,[14] showing a monomer unit with the inner (β-strands A′AHCF) and outer β-sheets (B′BGDE), which together form the β-sandwich of the monomer subunit; bottom loops BL1−4 and top loops TL1−4 are labeled accordingly. The disulfide bond connecting TL3 and TL4 is shown with yellow sticks. (A, bottom) Sketch showing the arrangement of the trimerization interface. β-Strands E and F of each monomer interact with the inner sheet of the adjacent monomer and in such a way assemble the trimer. Three tumor necrosis factor receptors (TNFR), represented by gray ellipsoids, can interact with one TNFα trimer. The interaction takes place at each intrasubunit groove and is mediated via contacts to TL1, TL2, and BL4. (B) Two-dimensional (2D) NMR spectrum using [^{1}H,^{15}N] transverse relaxation optimized spectroscopy (TROSY) of 1 mM [^{13}C,^{15}N]-labeled TNFα in 100 mM phosphate-buffered saline (PBS), pH 7.4, recorded at 310 K at 700 MHz; assigned residues are marked with a cross and, if resolved, are labeled with amino acid and residue number; 98.4% of the observable backbone signals are assigned (Supporting Information). (C) Sequence-specific combined chemical shift deviations (CCSD) of C$^\alpha$ and C$^\beta$ resonances from their respective random coil values; positive CCSD are indicative for α-helix, negative CCSD for β-sheet.[16] Secondary structure motifs of the crystal structure are indicated at the top: β-strands (black), β-turn (violet), and 3^{10}-helix (pink). (D, left) H/D exchange data reporting on solvent accessibility of backbone amides of TNFα in solution: fast-exchanging (green) and slowly exchanging (blue) NH protons as well as nonassigned (gray) residues are color-coded onto one TNFα monomer. Observed [^{1}H−^{1}H] nuclear Overhauser effects (NOEs) between amide protons (dashed lines) confirm the tertiary structure. The N- and C-termini are marked. (D, right) Three observed backbone ^{1}H−^{1}H amide−amide NOEs (dashed lines) correspond to distances larger than 5 Å in the crystal structure: V13−V41 (6.1 Å), S85−E131 (5.7 Å), and F64−L142 (5.8 Å). The corresponding amino acids are shown as sticks and labeled with name and residue number. These three violations can be explained by a prolongation of the secondary structural motifs by one residue. The crystal structure (PDB 1TNF)[14] was used for all figures. The N- and C-termini are marked when helpful for clarity.

the PPI site were proposed, but none of them has yet reached therapeutic usage.[13,26,28−33] For one small-molecular inhibitor, SPD304,[13] crystallographic data have elucidated the complex with TNFα, establishing the binding site at the trimerization interface and suggesting inactivation through disruption of the oligomeric state. However, targeting the PPI remains a challenge, especially due to the lack of prior knowledge about the detailed mechanism of inhibition at atomic resolution in solution.

In this study, we investigate the structural and dynamic features of TNFα in its active and inactivated forms, primarily by NMR spectroscopy. We present the first characterization of TNFα in solution at atomic resolution. We propose a model where trimer disruption is not a prerequisite for inhibition of TNFα, but rather differential dynamics controls its activity.

RESULTS

NMR Assignments and Comparison to Crystal Structure. TNFα represents a challenging case for NMR assignments due to its rather large size (51 kDa) and unfavorable dynamic properties. The conventional approach, using transverse relaxation optimized spectroscopy (TROSY)-type experiments[34] and perdeuteration[35] as applied for larger systems,[36] was hampered by the intrinsic dynamics of TNFα, which are manifested already in the [^{1}H,^{15}N]-TROSY spectrum in the form of exchange-broadened and missing resonances (Figure 1B). Thus, additional strategies were used, including selective amino acid type unlabeling[37] and site-specific mutations. With this combined approach, nearly all of the visible signals in the [^{1}H,^{15}N]-TROSY spectrum could be assigned (Figure 1B). Missing resonances in the fingerprint spectra correspond to the N-terminus, loops TL3 and TL4 around the disulfide bond, part of β-strand C of the interface (Figure 1A), and a RRA sequence in TL1 that mediates receptor binding. The solution NMR data were then compared to the crystal structure of TNFα. C$^\alpha$ and C$^\beta$ chemical shifts,[16] NMR proton/deuterium (H/D) exchange data of the backbone amide protons, and nuclear Overhauser effect (NOE) data revealed that the pattern of secondary structure elements in solution agrees with the crystal structure of TNFα (Figure 1A). However, two residues at the beginning of β-strand E do not show typical β-sheet backbone dihedral angle characteristics in solution (Figure 1C), and residue G24 shows a high amide proton exchange protection factor in solution despite being part of the flexible loop TL1 in the crystal structure. On the basis of carbon chemical shifts and the NOE pattern in ^{1}H−^{15}N−^{1}H NOE spectra, G24 seems to be involved in a short helical turn. Otherwise, all identified amide [^{1}H−^{1}H]-NOEs are consistent with the tertiary structure of TNFα in the crystal[14] (Figure 1D). These observations suggest that the crystal structure represents a good structural model of free TNFα in solution.

DOI: 10.1021/jacs.7b05050
J. Am. Chem. Soc. 2018, 140, 167−175

Active Tumor Necrosis Factor α Is a Highly Dynamic Trimeric Protein. We used NMR ^{15}N relaxation experiments to provide the basis for a dynamic characterization of TNFα in solution. Longitudinal (R_1) and transverse (R_2) relaxation rates and {^{1}H}−^{15}N heteronuclear nuclear Overhauser effect (hetNOE) experiments were recorded for active TNFα at three magnetic fields with 500, 600, and 700 MHz ^{1}H frequency (Figure 2). With the assumption of isotropic reorientation, correlation times τ_c of 25.6, 25.1, and 24.1 ns were obtained for TNFα at the three magnetic fields, respectively, compatible with a trimer (expected $\tau_c \approx 22$ ns).[38] The ^{15}N relaxation data at multiple magnetic field strengths were subjected to model-free analysis providing site-specific dynamic information for every amide bond vector relative to the global rotational diffusion tensor.[39,40] The diffusion tensor was determined based on the ratios R_2/R_1 of the most rigid residues with TNFα crystal structure as structural model (PDB 1TNF).[14,41] A prolate axially symmetric diffusion tensor was obtained, in good agreement with the symmetric nature of trimeric TNFα. The ^{15}N relaxation data (R_1, R_2, and hetNOE) were subsequently interpreted relative to the diffusion tensor with the model-free formalism by use of either a single or simultaneously all three magnetic fields.[42,43] This approach yields a generalized order parameter S^2, characterizing the extent of NH bond vector motion in the pico- to nanosecond time scale (S^2 ranges from 1 for a rigid vector to 0 for unrestricted motion) and an internal correlation time τ_e associated with this motion. Possible additional slower dynamics can be observed, either by the presence of slower motional modes (still faster than the reorientational correlation time τ_c) or by the presence of additional contributions (R_{ex}) to R_2, indicative of slower conformational exchange on the micro- to millisecond time scale (Figure 2). The β-sheets represent the most rigid part, with an average S^2 of 0.92, while residues in the loop regions have smaller values. Lowest order parameters and elevated τ_e values are found for residues in TL1, TL4, β-strand A′, and receptor binding sites, indicative of a higher degree of internal dynamics. Evidence for slower exchange contributions is seen for residues within the outer β-strand G and the β-sheet (strands H, C, and F) forming the trimer interface, suggesting the presence of slow time scale motions between the three monomers.

Interference with the Protein−Protein Interface Alters the Dynamics. Investigation of TNFα in solution revealed substantial dynamic motional rearrangements upon allosteric inhibition by interference with the PPI. The interface was perturbed by two different means: either by interaction with the small-molecule inhibitor SPD304, shown to bind at the trimerization interface and known to inactivate TNFα,[13,44−46] or by site-directed mutagenesis of residues at the trimerization interface known to preclude receptor binding, leading to TNFα inactivation.[11,12] In total seven TNFα mutants were constructed: four of the mutations are located at the trimerization interface (L57Y, Y59A, Y119S, and G121A interface mutants), and three are located in loop TL3 (T72A), in β-strand D (T89A), and at the C-terminal end of β-strand E (I97A). The specific mutants Y59A and Y119S were chosen on the basis of their very potent TNFα response inhibition.[12] While residue Y119 forms the most intimate contact at the trimer interface, Y59, L57, and G121 are also known to assist in trimer formation and to bind to SPD304.[13] Mutations T72A, T89A, and I97A are expected not to interfere with SPD304 binding nor cause trimer disruption and thus serve as negative controls.

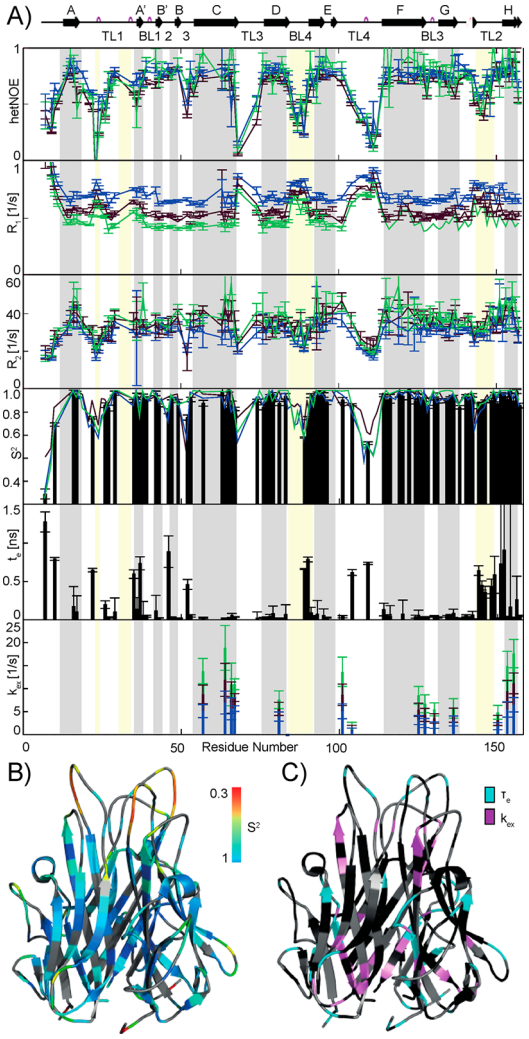

Figure 2. Backbone dynamics of TNFα in solution. (A) From top to bottom: {^{1}H}−^{15}N heteronuclear NOE (hetNOE), longitudinal (R_1), and transverse (R_2) relaxation rates, followed by the parameters derived from model-free analysis including order parameter (S^2) and time scales of motion (τ_e) and exchange contributions (k_{ex}). The measurements were performed at three magnetic field strengths: 500 (blue), 600 (red), and 700 MHz (green). Model-free parameters derived from simultaneous analysis of the three field strengths are shown as black bars, while order parameters derived from independent analysis of the three magnetic fields are color-coded as for the data. Exchanges contributions k_{ex} were derived from simultaneous analysis of the three fields, plotted with dependence on each of the three fields separately, and color-coded accordingly. β-Strands are highlighted with a light gray background, and regions mediating receptor binding are shaded light yellow.[11,12,17] At the top, secondary structure motifs of the crystal structure are depicted as in Figure 1C. (B, C) TNFα motions mapped onto the crystal structure (PDB 1TNF).[14] (B) Amplitudes of the pico- to nanosecond backbone NH motions, with rainbow color-coding for the general order parameter S^2 from rigid (S^2 = 1, blue) to flexible (S^2 = 0.3, red). (C) Amide moieties with internal motions on the nanosecond time scale (between 0.25 and 1.5 ns) (cyan) and with exchange contributions in the micro- to millisecond time scale (purple). Residues not experiencing any fast internal motions or chemical exchange are colored in black; gray indicates residues for which the relaxation parameters could not accurately be determined.

First, TNFα was titrated with increasing amounts of SPD304, and changes in TNFα were monitored by [^{1}H,^{15}N] heteronuclear single quantum coherence (HSQC) spectra (Figure 3

DOI: 10.1021/jacs.7b05050
J. Am. Chem. Soc. 2018, 140, 167−175

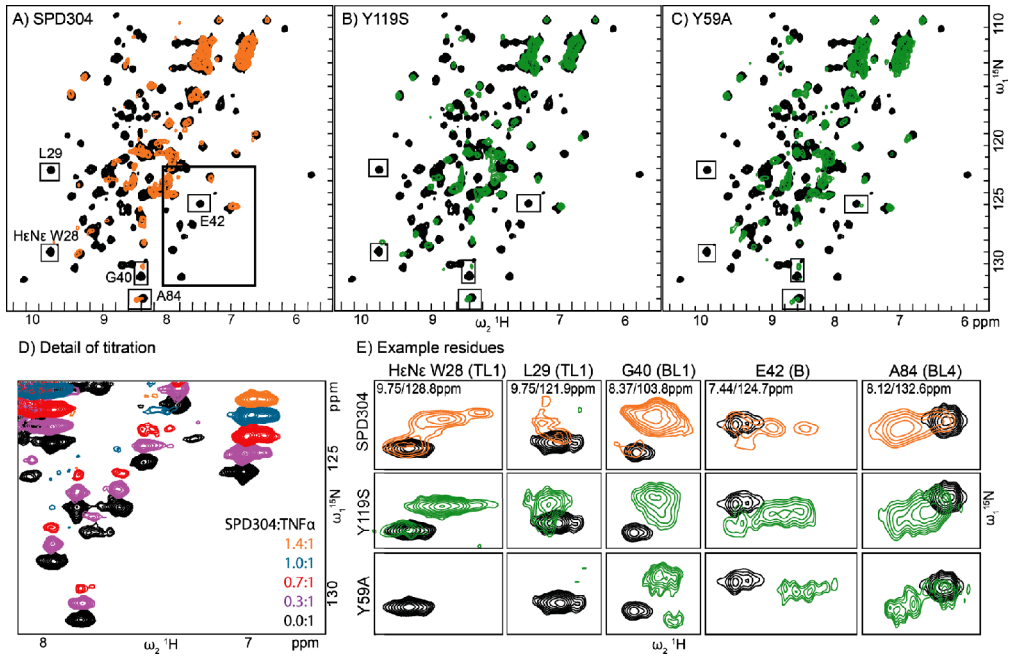

Figure 3. Conformational fluctuations in TNFα with perturbed protein−protein interface (PPI). (A) [^{1}H,^{15}N]-HSQC spectrum of native TNFα (black) overlaid to a spectrum of TNFα with SPD304 at a molar ratio of 1:1.4 (orange), measured on a 600 MHz spectrometer. The large box marks the area shown enlarged in panel D. The small boxes labeled with amino acid type and residue number indicate representative examples of resolved residues showing slow exchange between different conformations; these residues are depicted enlarged in panel E. Residue G40 is aliased in the ^{15}N dimension. (B) Same as in panel A but with superposition of native TNFα (black) and mutant Y119S (green). (C) Same as in panel B but with superposition of native TNFα (black) and mutant Y59A (green). (D) Spectral changes in spectra of TNFα upon titration with SPD304 with molar ratios (SPD304:TNFα) of 0 (black), 0.3 (violet), 0.7 (red), 1.0 (blue), and 1.4 (orange); for clarity, the spectra are overlaid with a small offset of 0.6 ppm in the ^{15}N dimension (^{15}N scale is correct for the black spectrum). A detailed region of the [^{1}H,^{15}N] spectrum is shown here; Figure S1 presents the full and expanded spectrum. (E) Boxed regions in panels A−C, plotted enlarged and with lower contour levels; residues are indicated on top with their secondary element in brackets; chemical shifts (ω_2/ω_1) are given in the top row.

and Figure S1). Upon addition of SPD304, the resonances throughout the spectrum broaden significantly, except for those corresponding to the loop regions or the small β-strand B′ (Figure 4 and Figure S2). Additionally, for numerous resonances (i.e., R138, A84, HεNε W28), the overall shape changes or new resonances in close proximity appear. Finally, a few amide resonances (i.e., A22) slightly change their combined chemical shift (ca. 0.06 ppm). (Figure 3D and Figure S2). These observations provide strong evidence for multiple stable conformations in slow to intermediate exchange when the PPI of TNFα is disturbed. Notably, these changes are not restricted to the trimerization interface. While the loss of intensity spans mainly the trimerization interface, the appearance of multiple peak maxima also includes residues in the loop region mediating receptor binding (Figure 3 and Figure S2).

On the basis of newly detected extensive motions in inhibited TNFα, we decided to study conformational changes induced in the PPI for the seven mutants described above. The four mutations at the trimer interface produced NMR spectra of striking similarities upon SPD304 titration (Figure 4). Interestingly, the mutation of the most proximal contact (Y119) resembles more closely the spectrum observed at high ratios of SPD304:TNFα, while mutations of PPI residues further from the interaction site (Y59 and G121) are more similar to those at lower SPD304 concentrations (Table S1). This strongly suggests that SPD304 interferes with the trimerization interface also in solution. On the contrary, alanine substitution mutants of residues remote from the trimer interface (negative controls) do not induce global conformational changes and have only local effects (Figure 4). Collectively, these results show that distortion of the interface by mutation or interaction with SPD304 leads to global dynamic fluctuations among multiple conformational states on the intermediate to slow (micro- to millisecond) time scale.

Global Structural Characteristics Are Retained upon Interference with the Protein−Protein Interface. The impact of disturbing the PPI on the oligomeric state was investigated by TRACT (transverse relaxation optimized spectroscopy for rotational correlation time)[47] NMR relaxation experiments with active TNFα, the complex TNFα/SPD304, and the most strongly disrupting mutant, Y119S. Analysis of the TRACT data resulted in average isotropic rotational correlation times τ_c of 22.5 ± 5.1 ns for TNFα/SPD304, 19.6 ± 0.98 ns for Y119S mutant, and 22 ± 2.8 ns for native TNFα (Figure 5C), in agreement with a preserved trimeric state. Additionally, the TRACT experiment confirmed the previously observed increase in conformational exchange by faster-decaying relaxation rates for the PPI perturbed forms. Since the high concentration of TNFα in the NMR samples could favor oligomerization, the oligomeric state of TNFα was further probed at lower concentrations by dynamic light scattering (DLS) and size-exclusion chromatography (SEC) (Figure S3 and Tables S2 and S3). These measurements provided hydrodynamic diameter and retention volume of 6.5 ± 1.5 nm and 11.2 mL for TNFα and 6.4 ± 1.4 nm and 11.08 mL for TNFα/SPD304, both consistent with a trimeric form. Moreover, multiangle light scattering (MALS), analytical ultracentrifugation (AUC), nanoelectrospray ionization mass spectrometry (nanoES-MS), cross-linking, and MicroScale Thermophoresis (MST) measurements further support a trimeric state for TNFα in both the absence and

DOI: 10.1021/jacs.7b05050
J. Am. Chem. Soc. 2018, 140, 167−175

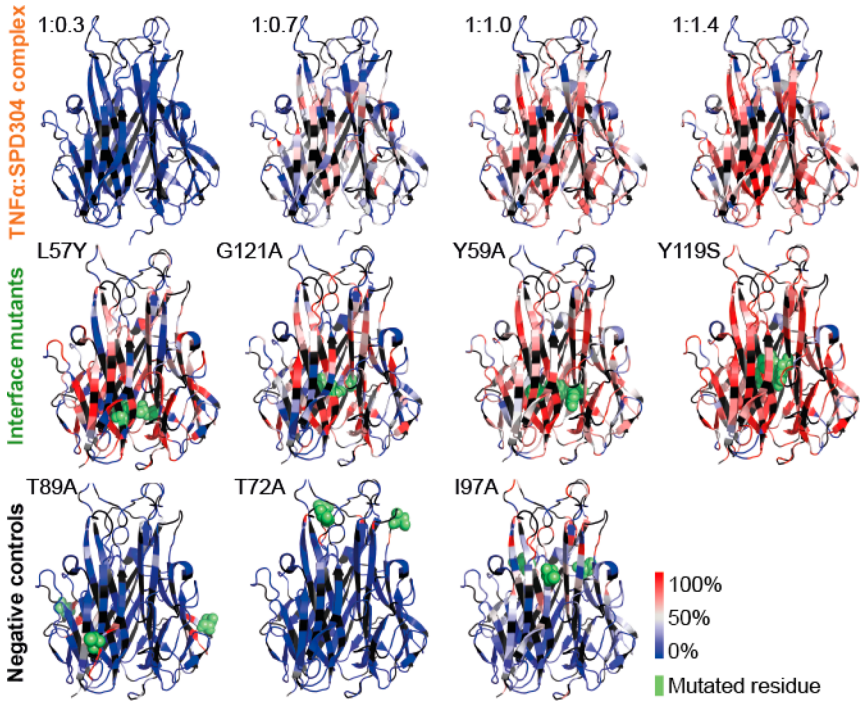

Figure 4. Intensity changes in [^{1}H,^{15}N]-HSQC spectra suggest similarities between the interface mutants and TNFα in complex with SPD304. Relative intensity changes plotted on the crystal structure (PDB 1TNF)[14] using the color code blue (0%) → white (50%) → red (100%); residues that are not assigned or overlapping are marked in black. (Top row) Native TNFα in the presence of increasing amounts of SPD304 (ratios given above the structures). (Middle row) Interface mutants of TNFα (mutations given above the structures) in comparison to native TNFα; green spheres indicate backbone and side-chain atoms of the residues mutated. (Bottom row) Same as middle row for mutations outside the PPI. A quantitative comparison is found in Table S1.

presence of SPD304 (Figures S3−S6). Additionally, neither DLS nor SEC performed on different interface mutants could reveal a change in the quaternary structure (Tables S2 and S3).

Possible changes in the secondary and tertiary structures of TNFα with perturbed interface were examined by ultraviolet circular dichroism (UV CD) and NMR H/D exchange experiments. Comparison of far-UV CD spectra of Y119S mutant and native TNFα revealed similar dichroic absorbances suggesting highly similar secondary structures, as confirmed by the negative band at 220 nm for both proteins, indicative of a high β-sheet content (Figure 5A). For TNFα/SPD304, the presence of dimethyl sulfoxide (DMSO; to solubilize SPD304) prohibits comparative CD spectra in the far-UV region. Therefore, the secondary structure of TNFα/SPD304 was investigated by NMR H/D exchange experiments. Only five residues, clustered at the top and bottom of the innermost β-strands, show elevated H/D exchange rates compared to native TNFα (Figure S7), indicating the preservation of β-sheet structure with a possible loosening at the trimerization interface due to binding of SPD304.

Near-UV CD spectra (Figure 5B) that report on the tertiary structure can be used as a fingerprint spectrum of TNFα.[10,48] Upon interaction with SPD304, the main maxima are present, indicating that TNFα overall conserves its tertiary structure. However, the main maxima are slightly shifted and associated with a decrease in dichroic absorption in the region 294.5−275 nm, usually related to a more relaxed environment and increased flexibility of a tyrosine or tryptophan side chain. Furthermore, an increased absorbance in the range 255−275 nm is observed that might be attributed to SPD304 experiencing an asymmetric environment when bound or to more restricted dynamics in phenylalanine residues of the protein. Our data suggest that disturbing the PPI of TNFα leads to local loosening of the tertiary structure, probably at the PPI, a characteristic often also associated with molten globule-like states. The molten globule-like nature of PPI-disturbed TNFα was tested by fluorescence spectroscopy with an 8-anilino-1-naphthalenesulfonic acid (ANS) assay[49] (Figure S8). Molten globules typically enhance ANS fluorescence intensity and shift the maximum toward lower wavelengths. This effect was observed for both TNFα/SPD304 and Y119S mutant. However, the strong interaction of SPD304 and ANS precluded a quantitative comparison of the two perturbations of the PPI. For Y119S, the effect remains much lower than for TNFα under conditions reported to mimic a molten globular TNFα (1 M guanidinium chloride).[50] Interestingly, Y59A does not induce such a shift, in agreement with previous NMR experiments indicating that this mutation induces less severe perturbation of the PPI than Y119S. These findings suggest that PPI-perturbed TNFα does not behave like a classical molten globule but that the appearance of interfacial loosening induces partial characteristics associated with a molten globular state. Overall, these experiments show that, upon perturbation of the PPI, TNFα conserves its oligomeric state and its secondary and mainly its tertiary structure, while dynamic conformational rearrangements occur.

Destabilization of the Protein−Protein Interface Affects Receptor Binding by Changes in Dynamics. Residues located in three loops, TL1, TL2, and BL4 (Figure 1A), mediate the interaction of TNFα with its receptors.[11,12,17] Despite strong exchange broadening in NMR spectra of TNFα with perturbed PPI, residues mediating receptor binding in TL2 and BL4 remain observable. The structural and dynamic properties of these residues were compared for native and PPI-perturbed TNFα (Y119S and TNFα/SPD304) to find

DOI: 10.1021/jacs.7b05050
J. Am. Chem. Soc. 2018, 140, 167−175

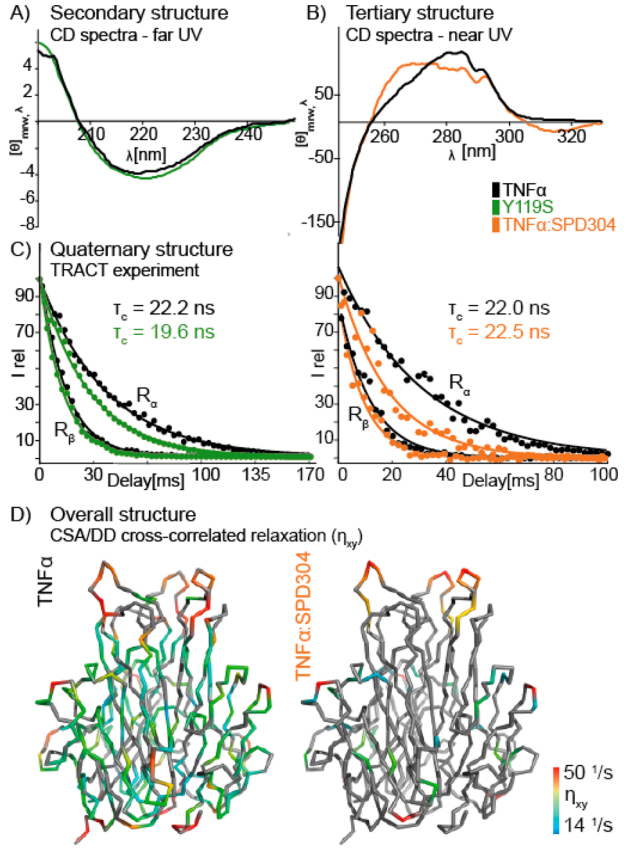

Figure 5. Structural characteristics of TNFα are preserved when the PPI is perturbed. (A) Circular dichroic (CD) spectra in the far-UV region (200−250 nm) for 0.178 mg/mL native TNFα (black) and 0.427 mg/mL Y119S mutant (green), reporting on the secondary structure; the dichroic absorbance is given in 10^3dec·cm^2·dmol^{-1}. (B) CD spectra of 300 μM TNFα (black) and an equimolar complex of TNFα and SPD304 (orange) in the near-UV region, reporting on tertiary structure; the measurements were repeated three times, and the dichroic absorbance is given in dec·cm^2·dmol^{-1}. (C, left) TRACT data (600 MHz) reporting on the quaternary structure of 600 μM TNFα (black) (τ_c = 22.2 ns, R_α = 24.27 Hz, R_β = 63.41 Hz) and of 600 μM Y119S (green) (τ_c = 19.6 ns, R_α= 32.43 Hz, R_β = 70.39 Hz). (C, right) TRACT data (750 MHz) reporting on the quaternary structure of 230 μM TNFα (black) (τ_c = 22.0 ns, R_α = 32.36 Hz, R_β = 85.42 Hz) and that of TNFα/SPD304 complex (1:1.4) (orange) (τ_c = 22.5 ns, R_α = 54.23 Hz, R_β = 108.60 Hz). (D) TNFα and TNFα/SPD304 exhibit similar fast time scale motions. The cross correlation rates η_{xy} between the amide chemical shift anisotropy (CSA) and the dipol-dipole interaction (DD) in the amide moiety are color-coded onto the crystal structure of TNFα (left) and the complex TNFα/SPD304 (1:0.75) (right) with a rainbow gradient from cyan (rigid, 14 s^{-1}) to red (flexible, 50 s^{-1}).[51] Backbone amide moieties that were missing in the NMR spectra, not assigned, overlapped, or with an error >15% are colored gray.

evidence for an explanation why distorting the PPI reduces the TNFα response.

To this end, amide three-dimensional (3D) ^{15}N-resolved [^{1}H,^{1}H]-NOESY data were used to detect possible changes in the local structure of the loop region provoked by perturbation of the interface. No differences in NOE patterns were found for different forms, indicating the absence of significant structural changes in TL2 and BL4 upon destabilization of the PPI (Table S4).

In addition to residues in TL2 and BL4, residues in TL1 also mediate interactions with the receptor.[11,12,17] However, resonances of these residues are not observable in any TNFα forms used in this study. To probe structural changes in TL1, we used trypsin digestion with the trypsin-sensitive RRA sequence (R31−A33) in TL1.[41] The efficiency of digestion was used to report on structural changes in TL1 upon distortions of the PPI (Figure S9). No significant differences could be observed between PPI-perturbed and nonperturbed forms of TNFα, implying no structural rearrangement in this loop region.

The poor spectral properties of PPI-perturbed TNFα preclude accurate measurements of NMR relaxation rates necessary for a detailed characterization of its conformational dynamics. Alternatively we measured cross-correlated relaxation (η_{xy}) resulting from the interference between dipole−dipole (DD) and chemical shift anisotropy (CSA) relaxation mechanisms. These experimentally more accessible quantities can be used to probe amplitudes of fast conformational dynamics, albeit at reduced precision.[51] Nevertheless, good agreement between the dynamic information extracted from cross-correlated relaxation and the previously obtained model-free order parameters was obtained for free TNFα (Figures 2 and 5). Cross-correlated relaxation constants were also measured on TNFα in the presence of SPD304, including the residues observable by NMR in TL2 and BL4 loops (Figure 5). These measurements did not indicate any systematic dynamic changes at the fast time scale in the presence of SPD304. Although, observed alteration of the NMR resonances in the receptor-binding region upon perturbation of the PPI, indicate the presence of a slow conformational dynamic transition (Figures 3 and 4).

Collectively, these data (summarized in Table S4) suggest a destabilized PPI retains a similar 3D arrangement and local motions for the loop regions that mediate receptor binding, implying that each monomer is limitedly affected in its overall fold by perturbation of the PPI. This suggests the observed increased conformational dynamics results from a loosening of the PPI, allowing the different monomers to sample different relative conformations. As the receptor-binding region spans over two monomers, the appearance of this intersubunit motion could affect the binding properties to the receptor while preserving monomer integrity (Figure 6). This model is consistent not only with our NMR data but also with the diverse biophysical techniques used (vide supra).

To further test our model, the in vivo activity of cross-linked trimeric TNFα in the presence and absence of SPD304 was investigated (Figure S10). We observed similar activity in a dose-dependent cell cytotoxicity assay in mouse fibroblast cells of TNFα and cross-linked TNFα, but we noted reduced activity of TNFα/SPD304 (1:100) and trimeric cross-linked TNFα/SPD304 (1:100), while no effect of SPD304 alone was measured. These results suggest that SPD304 can inhibit a covalently bound trimeric form of TNFα that remains unaffected by a monomer−trimer equilibrium, possibly appearing at low in vivo concentrations. These results further support our proposed model mechanism.

DISCUSSION

Although the static three-dimensional crystal structures of native TNFα[14] and of TNFα in complex with the small molecule SPD304[13] provide some insight into the understanding of TNFα, our results demonstrate that dynamic motions are key features of this inactive form of TNFα. Here we show that the

DOI: 10.1021/jacs.7b05050
J. Am. Chem. Soc. 2018, 140, 167−175

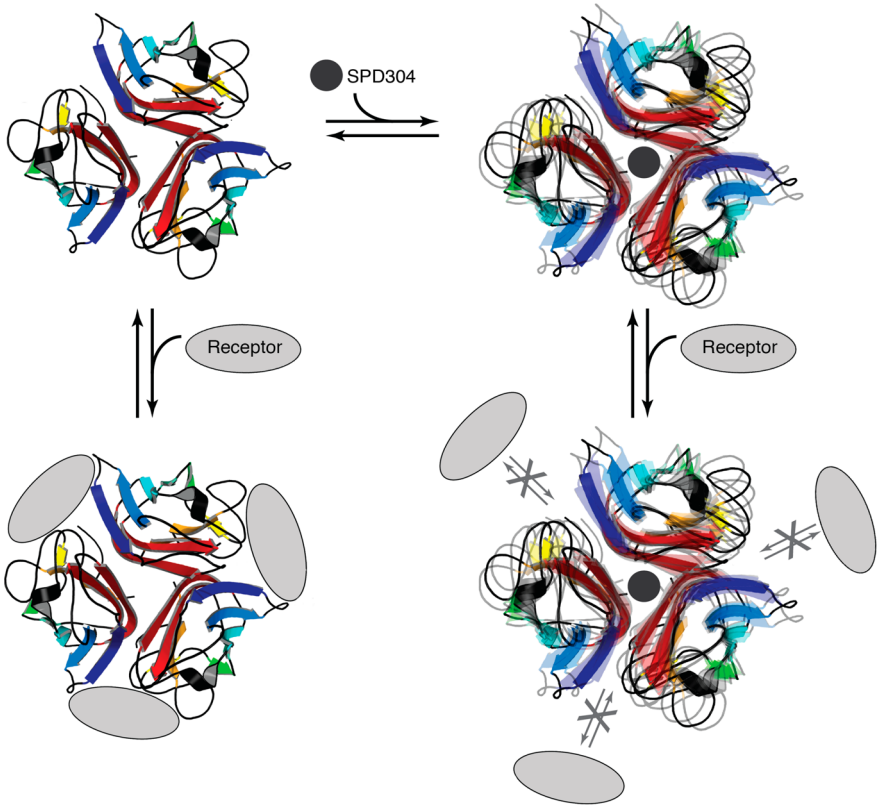

Figure 6. Proposed mechanism for TNFα inactivation upon perturbation of its PPI. Native TNFα exists as a homotrimer and is capable of interacting with the receptor. The interaction with SPD304 (shown as a black circle) provokes increased dynamics in the PPI that loosens the interaction between the TNFα monomers and leads to relative motions between them. The receptor-binding interface spans over two monomers, and consequently the relative motion between the monomers reduces the capability of TNFα to interact with the receptor, without global structural changes of each monomer.

published crystal structure is a valid model for native TNFα in solution. Additionally, we clearly demonstrate that residues involved in the interaction with the receptors of TNFα show high flexibility on the pico- to nanosecond time scale.

On the basis of the cocrystal structure, it was proposed that small-molecule inhibitors break up the trimeric form of TNFα to form a complex with a dimeric state.[13] Our data do not support this view, though they corroborate prior suggestions of the existence of an intermediate trimetric complex between TNFα and the small molecule SPD304.[13,44]

Our data show that perturbations of the PPI conserve the tertiary structure and trimeric state of TNFα despite inducing major changes in the energy landscape of the TNFα trimer. This modulation of conformational flexibility of TNFα was clearly revealed by the appearance of additional dynamics in the micro- to millisecond time scale after interference with the drug not only in the PPI but also in the receptor-binding region formed by two monomers. The highly dynamic nature of TNFα in complex with the small molecule SPD304, as observed by solution NMR, most likely prohibits the formation of crystals. Thus, the complex observed in the crystal may result from trapping of an alternative form favored by the crystalline environment.

The crystal structure between TNFα and SPD304 places the binding site at the lower part of the pore. Docking studies between this inhibitor and the trimeric form of TNFα showed interactions at the top end of the trimerization interface, proposing that further rearrangements are necessary for accessing the interface core.[52] Our results with the interface mutants are consistent with an interaction at the core of the trimer (Figure 4). Possibly, the high flexibility at the PPI upon interaction with SPD304 increases intersubunit mobility and allows access to the buried trimerization interface.

The activity of TNFα is known to crucially depend on the well-conserved interface residue(s) Y119 and/or Y59 without disruption of the oligomeric state.[11,12] These observations led to the conclusion that unobservable abnormalities are responsible for the inactivity of TNFα. Now, 25 years later, our data resolve this seemingly paradoxical case by providing novel insights on how the activity of TNFα is modulated by allosteric modifications at the PPI. The unobservable abnormalities in our model are drastic and global dynamic increases in subunit mobility in the trimeric TNFα.

Our studies of TNFα in solution at atomic resolution provide strong evidence that, upon perturbation of the PPI, the structure of each monomer along with the oligomeric state remains intact (Figure 5, Figures S3−S9, and Tables S2 and S3). We investigated the oligomeric state of TNFα down to nanomolar levels, a range approaching the concentration at which the activity of TNFα is measured in vivo. Our conclusions are based on detailed investigation of the key mutations (Y59A, Y119S) as well as interactions with SPD304, and additional mutations in the interface (L57Y, G121A) are in line with these conclusions. Furthermore, our data show that perturbation of the trimeric interface leads to a local increase in conformational exchange for residues at the trimerization interface. This loosening of the interface, build from the two innermost β-strands B and F of one monomer facing the inner β-sheet of the adjacent monomer

DOI: 10.1021/jacs.7b05050
J. Am. Chem. Soc. 2018, 140, 167−175

(Figure 1A), induces increased dynamics over the whole PPI, allowing the simultaneous existence of different heterogeneous conformational trimeric isomers. Ultimately, the dynamics of the intersubunit groove, which mediates receptor binding, is also affected (Figures 3 and 4 and Figure S2). We therefore conclude that an allosteric coupling mediated by conformational dynamics exists between the trimer interface and receptor-binding site: a change in interface dynamics will modulate the binding energetics to the receptor, explaining the decreased activity of TNFα (Figure 6). It seems that the aromatic rings of Y119 and Y59 act as locks and rigidify the TNFα quaternary structure. When perturbed by mutation or by drug binding, multiple interface contacts become possible, inducing global conformational consequences without destroying the trimeric form.

The idea that TNFα can exist as a trimer with increased flexibility and dynamics was previously suggested in studies on the folding pathway of TNFα, where the disassembly of TNFα happens via an intermediate trimeric molten globule.[48,50] Our analysis reveals that TNFα has some but limited characteristics of a molten globule-like state, resulting from loosening of the PPI while no evidence of significant loss of tertiary or quaternary structure could be observed.

In summary, we propose a mechanism where the key to TNFα inactivation lies in dynamic changes. When its interface is disturbed, TNFα remains trimeric but with a highly dynamic PPI. This increased dynamics propagates through the protein, altering the energy landscape of the receptor-binding domain, which impedes proper interactions. Our biophysical results reveal internal mobility as a further dimension in the regulation of TNFα activity, a mechanism that might be applicable for other proteins with similar oligomeric architecture. The model mechanism based on in vitro data was further supported by in vivo experiments. We expect our results to have significant implications for assessing possibilities to regulate TNFα and therefore for opening avenues for novel anti-TNFα therapeutic developments.

MATERIALS AND METHODS

Here only general procedures are described; more detailed descriptions can be found in the Supporting Information.

Sample Preparation. Human TNFα (UniProtKB P01375), production was performed as previously described.[44] Protein purity and molecular weight was confirmed by ES-MS, and the activity of TNFα was verified by a cytotoxicity assay using mouse fibroblast cells (LM, American Type Culture Collection).[53] The melting temperatures of TNFα and the Y119S mutant were obtained by use of SYPRO Orange.[54]

NMR Spectroscopy. NMR samples were prepared in 150 mM 3-(*N*-morpholino)propanesulfonic acid (MOPS) and 50 mM ammonium acetate buffer, pH 7.2, and measured at 310 K, unless otherwise stated.

NMR Assignment. Resonance assignments were obtained with 1 mM uniformly $^{2}H,^{13}C,^{15}N$-labeled TNFα in 100 mM PBS in 90%/10% H_2O/D_2O, pH 7.4, using TROSY versions of three-dimensional NMR experiments[34,55] at 600, 700, and 900 MHz. TNFα chemical shift assignments have been deposited in the Biological Magnetic Resonance Data Bank (BMRB) under entry code 27266.

H/D Exchange Experiments (700 MHz). ^{15}N-Labeled TNFα was lyophilized overnight and quickly dissolved in 100% D_2O right before the measurement. Changes in signal intensities were monitored by 2D $[^{1}H,^{15}N]$-HSQC spectra over the time range from 10 min after dissolution to 17 days.

^{15}N Relaxation Measurements (500/600/700 MHz). R_1 and R_2 relaxation rates and hetNOE experiments were acquired at all three fields on a ^{15}N-labeled 1.2 mM sample by use of standard pulse sequences.[56] The cross-correlated relaxation rates η_{xy} (700 MHz) were measured on a 1.2 mM ^{15}N-labeled TNFα sample and a 0.4 mM TNFα/SPD304 (1:0.75) complex by use of published pulse sequences.[51] Data were processed and analyzed by use of TopSpin 3.2 and Dynamic Center (Bruker Biospin, Karlsruhe, Germany). Fitting of the rotational diffusion tensor and model-free analysis were performed with the program TENSOR v2.[42]

Titrations Monitored by $[^{1}H,^{15}N]$-Heteronuclear Single Quantum Coherence Spectroscopy (600/750 MHz). SPD304 (Cayman, Ann Arbor, MI)[44,46] was titrated stepwise to 230 μM $[^{13}C,^{15}N]$-labeled TNFα including ratios 0, 0.3, 0.7, 1.0, 1.4 (SPD304/TNFα). $[^{1}H,^{15}N]$-HSQC spectra were measured for all titration steps. Titrations were also performed for mutants G121A, Y59A, Y119S, T89A, T72A, I97A, and L57Y. Influences of the presence of DMSO-d_6, of a change in pH, and of the presence of N-terminal $(His)_6$ tag on the observed $[^{1}H,^{15}N]$ spectra were investigated and could be excluded.

Transverse Relaxation Optimized Spectroscopy for Rotational Correlation Time Experiments. TRACT[47] spectra were obtained with ^{15}N-labeled protein samples: 230 μM TNFα and 230 μM:300 μM TNFα/SPD304 complex (750 MHz) and 600 μM TNFα and 600 μM Y119S (600 MHz).

Oligomeric State. DLS experiments were performed on 60 μM TNFα, 60 μM Y119S mutant, and 60 μM TNFα in the presence of 300 μM SPD304. SEC was performed on 100−200 μM TNFα, mutant versions, and TNFα/SPD304 (1:1.4). The protein was monitored at 280 nm; the DMSO concentration was identical for all samples. NanoES-MS was conducted on 4.5 μM TNFα, TNFα/SPD304 (1:3), and Y119S. MST and cross-linking were performed on TNFα in the presence and absence of SPD304, over the nanomolar concentration range.

Circular Dichroism. Optical activity was measured on a Jasco J-715 spectropolarimeter at 30 °C. Near-UV (240−330 nm) spectra were acquired at a protein concentration of 300 μM. Either 2.5% DMSO or 300 μM SPD304 to a final DMSO concentration of 2.5% was added. Far-UV (200−250 nm) spectra were measured on a TNFα sample of 0.18 mg/mL and on the mutant Y119S (0.43 mg/mL) in 100 mM PBS buffer, pH 7.4.

ASSOCIATED CONTENT

Supporting Information

The Supporting Information is available free of charge on the ACS Publications website at DOI: 10.1021/jacs.7b05050.

Additional text with detailed materials and methods; 10 figures showing additional TNFα NMR characterization, AUC, DLS, MALS, H/D exchange, ANS, MST, cross-linking, cell assays, fluorescence, and trypsin digestion data; and four tables listing additional analyses of TNFα perturbation as well as TNFα NMR assignment (PDF)

AUTHOR INFORMATION

Corresponding Author

*gsw@mol.biol.ethz.ch

ORCID

Daniela Hofmann: 0000-0001-7073-0744

Notes

The authors declare no competing financial interest.

ACKNOWLEDGMENTS

We are grateful to Professor Rudi Glockshuber (ETH Zurich) for use of a CD spectrometer and to Maximilan Sauer (ETH Zurich) for providing technical assistance in performing CD and fluorescence measurements. We further thank Dr. Bolisetty Sreenath (ETH Zurich) for help with DLS experiments and Professor Raffaele Mezzenga (ETH Zurich) for use of his DLS equipment. We thank Professor Gebhard Schertler (PSI

DOI: 10.1021/jacs.7b05050
J. Am. Chem. Soc. 2018, 140, 167−175

Villigen) for use of his MALS and AUC equipment, and we thank Daniel Mayer and Dr. Rezabkova Lenka (both at PSI Villigen) for performing and analyzing AUC and MALS data, respectively. We thank Dr. Martin Blackledge (IBS, Grenoble) for providing TENSOR software allowing for multiple-field analysis. We also thank Dr. Erich Michel (UZH Zurich) for construction of the vector pEM1. We thank Susanne Mailand, Ahmed Moursy, and Roberto De Luca (all at ETH Zurich) for help with the cell-based assays and Professor Dario Neri (ETH Zurich) for providing the fibroblast cells. We further thank Professor Ruedi Aebershold (ETH Zurich) for cross-linker reactants and Dr. Rodolfo Cuiffa and Dr. Federico Uliana (both at ETH Zurich) for constructive discussions and enlightening information on the behavior of TNFα in vivo. We thank Professor Kaspar Locher (ETH Zurich) for use of the MST instrument. We also thank Professor Renato Zenobi (ETH Zurich) for access to nanoES-MS equipment and Agni Gavriilidou (ETH Zurich) for assistance in recording the experiments. Last but not least, we thank Dr. Michal Walczak (ITWM Basel) for helpful discussions. This research was supported by the Swiss National Science Foundation (Grant 144242).

REFERENCES

(1) Bradley, J. R. *J. Pathol.* **2008**, *214*, 149.
(2) Aggarwal, B. B.; Gupta, S. C.; Kim, J. H. *Blood* **2012**, *119*, 651.
(3) Kalliolias, G. D.; Ivashkiv, L. B. *Nat. Rev. Rheumatol.* **2015**, *12*, 49.
(4) Locksley, R. M.; Killeen, N.; Lenardo, M. J. *Cell* **2001**, *104*, 487.
(5) Idriss, H. T.; Naismith, J. H. *Microsc. Res. Tech.* **2000**, *50*, 184.
(6) Aggarwal, B. B. *Nat. Rev. Immunol.* **2003**, *3*, 745.
(7) Bodmer, J. L.; Schneider, P.; Tschopp, J. *Trends Biochem. Sci.* **2002**, *27*, 19.
(8) Smith, C. A.; Farrah, T.; Goodwin, R. G. *Cell* **1994**, *76*, 959.
(9) Smith, R. A.; Baglioni, C. *J. Biol. Chem.* **1987**, *262*, 6951.
(10) Wingfield, P.; Pain, R. H.; Craig, S. *FEBS Lett.* **1987**, *211*, 179.
(11) Yamagishi, J.; Kawashima, H.; Matsuo, N.; Ohue, M.; Yamayoshi, M.; Fukui, T.; Kotani, H.; Furuta, R.; Nakano, K.; Yamada, M. *Protein Eng., Des. Sel.* **1990**, *3*, 713.
(12) Zhang, X.-M.; Weber, I.; Chen, M.-J. *J. Biol. Chem.* **1992**, *267*, 24069 (http://www.jbc.org/content/267/33/24069.full.pdf).
(13) He, M. M.; Smith, A. S.; Oslob, J. D.; Flanagan, W. M.; Braisted, A. C.; Whitty, A.; Cancilla, M. T.; Wang, J.; Lugovskoy, A. a; Yoburn, J. C.; Fung, A. D.; Farrington, G.; Eldredge, J. K.; Day, E. S.; Cruz, L. a; Cachero, T. G.; Miller, S. K.; Friedman, J. E.; Choong, I. C.; Cunningham, B. C. *Science* **2005**, *310*, 1022.
(14) Eck, M. J.; Sprang, S. R. *J. Biol. Chem.* **1989**, *264*, 17595 (http://www.jbc.org/content/264/29/17595.full.pdf).
(15) Jones, E. Y.; Stuart, D. I.; Walker, N. P. *Nature* **1989**, *338*, 225.
(16) Wishart, D. S.; Sykes, B. D. *J. Biomol. NMR* **1994**, *4*, 171.
(17) Mukai, Y.; Nakamura, T.; Yoshikawa, M.; Yoshioka, Y.; Tsunoda, S.; Nakagawa, S.; Yamagata, Y.; Tsutsumi, Y. *Sci. Signaling* **2010**, *3*, ra83.
(18) Banner, D. W.; D'Arcy, A.; Janes, W.; Gentz, R.; Schoenfeld, H. J.; Broger, C.; Loetscher, H.; Lesslauer, W. *Cell* **1993**, *73*, 431.
(19) Machold, K. P.; Smolen, J. S. *Expert Opin. Biol. Ther.* **2003**, *3*, 351.
(20) Mauser, J. F.; Hyams, J. S. *Clin. Ther.* **1999**, *21*, 932.
(21) Keystone, E.; Van Der Heijde, D.; Mason, D., Jr.; Landewé, R.; Van Vollenhoven, R.; Combe, B.; Emery, P.; Strand, V.; Mease, P.; Desai, C.; Pavelka, K. *Arthritis Rheum.* **2008**, *58*, 3319.
(22) Smolen, J.; Landewé, R. B.; Mease, P.; Brzezicki, J.; Mason, D.; Luijtens, K.; van Vollenhoven, R. F.; Kavanaugh, A.; Schiff, M.; Burmester, G. R.; Strand, V.; Vencovský, J.; van der Heijde, D. *Ann. Rheum. Dis.* **2009**, *68*, 797.
(23) Pappas, D. A.; Bathon, J. M.; Hanicq, D.; Yasothan, U.; Kirkpatrick, P. *Nat. Rev. Drug Discovery* **2009**, *8*, 695.
(24) Hansel, T. T.; Kropshofer, H.; Singer, T.; Mitchell, J. A.; George, A. J. T. *Nat. Rev. Drug Discovery* **2010**, *9*, 325.
(25) Palladino, M. a; Bahjat, F. R.; Theodorakis, E. a; Moldawer, L. L. *Nat. Rev. Drug Discovery* **2003**, *2*, 736.
(26) Davis, J. M.; Colangelo, J. *Future Med. Chem.* **2013**, *5*, 69.
(27) Tristano, A. G. *J. Neurol.* **2010**, *257*, 1421.
(28) Chan, D. S.-H.; Lee, H.-M.; Yang, F.; Che, C.-M.; Wong, C. C. L.; Abagyan, R.; Leung, C.-H.; Ma, D.-L. *Angew. Chem., Int. Ed.* **2010**, *49*, 2860.
(29) Buller, F.; Zhang, Y.; Scheuermann, J.; Schäfer, J.; Bühlmann, P.; Neri, D. *Chem. Biol.* **2009**, *16*, 1075.
(30) Alzani, R.; Corti, A.; Grazioli, L.; Cozzi, E.; Ghezzi, P.; Marcucci, F. *J. Biol. Chem.* **1993**, *268*, 12526 (http://www.jbc.org/content/268/17/12526.full.pdf).
(31) Shah, B. A.; Chib, R.; Gupta, P.; Sethi, V. K.; Koul, S.; Andotra, S. S.; Nargotra, A.; Sharma, S.; Pandey, A.; Bani, S.; Purnima, B.; Taneja, S. C. *Org. Biomol. Chem.* **2009**, *7*, 3230.
(32) Choi, H.; Lee, Y.; Park, H.; Oh, D.-S. *Bioorg. Med. Chem. Lett.* **2010**, *20*, 6195.
(33) Luzi, S.; Kondo, Y.; Bernard, E.; Stadler, L. K. J.; Vaysburd, M.; Winter, G.; Holliger, P. *Protein Eng., Des. Sel.* **2015**, *28*, 45.
(34) Pervushin, K.; Riek, R.; Wider, G.; Wüthrich, K. *Proc. Natl. Acad. Sci. U. S. A.* **1997**, *94*, 12366.
(35) Venters, R. A.; Farmer, B. T., II; Fierke, C. A.; Spicer, L. D. *J. Mol. Biol.* **1996**, *264*, 1101.
(36) Tugarinov, V.; Hwang, P. M.; Kay, L. E. *Annu. Rev. Biochem.* **2004**, *73*, 107.
(37) Bellstedt, P.; Seiboth, T.; Häfner, S.; Kutscha, H.; Ramachandran, R.; Görlach, M. *J. Biomol. NMR* **2013**, *57*, 65.
(38) Ortega, A.; Amorós, D.; García De La Torre, J. *Biophys. J.* **2011**, *101*, 892.
(39) Lipari, G.; Szabo, A. *J. Am. Chem. Soc.* **1982**, *104*, 4559.
(40) Clore, G. M.; Szabo, A.; Bax, A.; Kay, L. E.; Driscoll, P. C.; Gronenborn, A. M. *J. Am. Chem. Soc.* **1990**, *112*, 4989.
(41) Cha, S. S.; Kim, J. S.; Cho, H. S.; Shin, N. K.; Jeong, W.; Shin, H. C.; Kim, Y. J.; Hahn, J. H.; Oh, B. H. *J. Biol. Chem.* **1998**, *273*, 2153.
(42) Dosset, P.; Hus, J. C.; Blackledge, M.; Marion, D. *J. Biomol. NMR* **2000**, *16*, 23.
(43) Rasheed, M.; Richter, C.; Chisty, L. T.; Kirkpatrick, J.; Blackledge, M.; Webb, M. R.; Driscoll, P. C. *Biochemistry* **2014**, *53*, 1092.
(44) Cubrilovic, D.; Barylyuk, K.; Hofmann, D.; Walczak, M. J.; Gräber, M.; Berg, T.; Wider, G.; Zenobi, R. *Chem. Sci.* **2014**, *5*, 2794.
(45) Chang, Y. J.; Hsu, S. L.; Liu, Y. T.; Lin, Y. H.; Lin, M. H.; Huang, S. J.; Ho, J. A. A.; Wu, L. C. *PLoS One* **2015**, *10*, No. e0120713.
(46) Edrissi, H.; Schock, S. C.; Hakim, A. M.; Thompson, C. S. *Brain Res.* **2016**, *1634*, 83.
(47) Lee, D.; Hilty, C.; Wider, G.; Wüthrich, K. *J. Magn. Reson.* **2006**, *178*, 72.
(48) Hlodan, R.; Pain, R. H. *FEBS Lett.* **1994**, *343*, 256.
(49) Semisotnov, G. V.; Rodionova, N. A.; Razgulyaev, O. I.; Uversky, V. N.; Gripas', A. F.; Gilmanshin, R. I. *Biopolymers* **1991**, *31*, 119.
(50) Hlodan, R.; Pain, R. H. *Eur. J. Biochem.* **1995**, *231*, 381.
(51) Tjandra, N.; Szabo, A.; Bax, A. *J. Am. Chem. Soc.* **1996**, *118*, 6986.
(52) Kim, O. T. P.; Le, M. D.; Trinh, H. X.; Nong, H. V. *Biophys. Physicobiol.* **2016**, *13*, 173.
(53) Corti, A.; Poiesi, C.; Merli, S.; Cassani, G. *J. Immunol. Methods* **1994**, *177*, 191.
(54) Niesen, F. H.; Berglund, H.; Vedadi, M. *Nat. Protoc.* **2007**, *2*, 2212.
(55) Kanelis, V.; Forman-Kay, J. D.; Kay, L. E. *IUBMB Life* **2001**, *52*, 291.
(56) Fushman, D.; Tjandra, N.; Cowburn, D. *J. Am. Chem. Soc.* **1999**, *121*, 8577.

DOI: 10.1021/jacs.7b05050
J. Am. Chem. Soc. 2018, 140, 167−175